ACS OMEGA

http://pubs.acs.org/journal/acsodf

Article

Effect of Water on Phenol Separation from Model Oil with Ionic Liquids Based on COSMO-RS Calculation and Experimental Study

Qian Liu, Jing Bi, and Xianglan Zhang*

Cite This: *ACS Omega* 2021, 6, 27368−27378

Read Online

ACCESS | Metrics & More | Article Recommendations | Supporting Information

ABSTRACT: Ionic liquids (ILs) are widely used in the extraction of phenolic compounds from low-temperature coal tar (LTCT). However, both ILs and LTCT contain a certain amount of water. The existence of water may have a remarkable impact on the phenol separation performance of ILs with different structures. In this work, the capacity and selectivity for *m*-cresol, as well as the solubility of cumene and dodecane in different IL−H_2O mixtures, were firstly calculated by the conductor-like screening model for real solvents (COSMO-RS) at infinite dilution. The calculation covers ILs with different anionic and anionic structures and different water contents. To explore the effect of water in IL on separation performance, 1-ethyl-3-methyl imidazolium acetate ([C_2mim][Ac]) was selected as the representative IL, and then the molecular interactions between the [C_2mim][Ac]−H_2O mixture solvent and solute (including *m*-cresol, cumene, and dodecane) were analyzed by COSMO-RS. The results indicated that both water and *m*-cresol could form hydrogen bonds with [C_2mim][Ac]. The competition between them leads to decreasing separation performance for *m*-cresol of the [C_2mim][Ac]−H_2O mixture with increasing water content. Moreover, through analyses of *m*-cresol extraction efficiency, distribution coefficient, selectivity, and entrainment of cumene and dodecane, the experimental results confirmed that the presence of water in [C_2mim][Ac] had a negative effect on the separation of *m*-cresol. The viscosity and UV−vis spectra of the [C_2mim][Ac]−H_2O mixture were also measured. Water in ILs should be removed as much as possible to ensure a better dephenolization effect and avoid phenol containing wastewater.

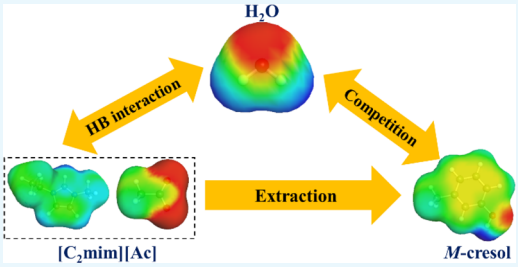

1. INTRODUCTION

Low-temperature coal tar (LTCT) is derived from the low-temperature pyrolysis of coal and contains a large amount of phenolic compounds, aromatic hydrocarbons, and aliphatic hydrocarbons.[1] Among them, the content of phenolic compounds is as high as 20−30% in LTCT.[1−4] They are important organic chemicals for producing phenolic resins, plant protectants, rubber antiagers, explosives, and so on in the chemical industry.[5−8] Moreover, the existence of phenolic compounds could reduce the stability of coal tar, increase hydrogen consumption in the subsequent processing, and produce phenolic wastewater.[9,10] Hence, it is essential to separate phenolic compounds from LTCT for further refining or application.

The traditional method to separate phenolic compounds from LTCT in the industry is the alkali wash method using a NaOH aqueous solution. Then, inorganic acids (such as H_2SO_4) are used to recover phenolic compounds.[11,12] However, this method not only consumes large amounts of acid and alkali but also causes corrosion to the equipment. Therefore, it is necessary to find a green separation method for recovering phenolic compounds from LTCT. In general, the method of organic solvent extraction has been applied to the separation of phenols.[13,14] In our previous research, Liu et al. used the UNIFAC and COSMO-SAC model to determine ethylene glycol as the suitable extractant for phenol separation from aromatic hydrocarbon, and liquid−liquid equilibrium (LLE) data of ethylene glycol + phenols + toluene were obtained at different temperatures.[15] This method has the advantages of simple operation and environmental protection. However, the low extraction efficiency of phenol is a major drawback of this method.

In recent years, many researchers have used ionic liquids (ILs) as extractants to solve the above problems. ILs have the advantages of structural designability, low vapor pressure, and high thermal stability, which have been applied to synthesis,[16] extractive distillation,[17−19] catalysis,[20] and extraction.[21,22] In the separation of phenolic compounds, Hou et al. used 1-butyl-3-methylimidazolium chloride ([C_4mim][Cl]) as the extractant; the extraction efficiency of phenol from hexane was up to 99.1%, and that from real coal liquefaction oil could reach 90%.[23] However, [C_4mim][Cl] is small in structure, easily dissolves in coal tar, and has a lower thermal decomposition temperature (150 °C). To solve this problem, Ji et al.

Received: August 8, 2021
Accepted: September 24, 2021
Published: October 8, 2021

synthesized six dicationic ionic liquids (DILs) to extract phenol from model oil. The thermal decomposition temperature of these DILs was higher than 200 °C, and the solubility in the model oil was less than 50 ppm.[24,25] Among them, the best extraction efficiency of *N*,*N*,*N*,*N*′,*N*′,*N*′-hexaethyl-propane-1,3-diammonium dibromide (HPDBr) could reach 97%. Nevertheless, these DILs still have two problems. First, the DILs contain halogen ions, which are corrosive to the equipment. Second, DILs are not conducive to mass transfer in industrial production because they are solid at room temperature. It is significant to find an extractant that has a high extraction efficiency, is liquid at room temperature, and has a low equipment loss.

Recently, our group screened 1-ethyl-3-methyl imidazolium acetate ([C_2mim][Ac]) through the conductor-like screening model for real solvents (COSMO-RS); the IL had the best extraction efficiency of *m*-cresol from model oil (98.85%) and recycling performance.[26] We also found that the shorter alkyl chain length of imidazole cation was favorable for extraction separation of *m*-cresol. Li et al. and Xu et al. synthesized 1-ethyl-3-methyl imidazolium thiocyanate ([C_2mim][SCN]) and 1-ethyl-3-methyl imidazolium lactate ([C_2mim][LAC]) as extractants to separate phenolic compounds from coal tar.[10,27] They also confirmed that hydrogen bonds are the main forces between ILs and phenolic compounds. However, we should note that these ILs easily absorb water, and they contain a part of water due to the presence of water vapor in the air. On the other hand, LTCT also contains some water. The existence of water has a great influence on the physical properties of ILs, such as density and viscosity.[28,29] More importantly, the existence of water can affect the extraction efficiency of ILs for phenolic compounds. Ren et al. reported that the extraction efficiency of choline chloride (ChCl) decreased from 92.4 to 83.8% when the water content of model oil increased from 1 to 7%.[30] Ji et al. found that when the water content of tetraethylammonium L-alanine ([Et_4N][L-Ala]) is less than 10%, the extraction efficiency of phenol hardly decreases.[31] The results show that water has different effects on ILs with different structures. In addition, water also has a certain solubility in hydrophobic ILs.[32,33] For the extraction of aromatics from aliphatics, Yao et al. reported that hydrophobic DIL [$C_5(mim)_2$][NTf_2]$_2$ containing less than 2 wt % water not only had a great decrease in viscosity but also had high distribution coefficient (D) and selectivity (S) at the same time.[34] However, the effect of water in hydrophobic ILs on the separation process of phenolic compounds is rarely reported.

Based on the current research status, it is necessary to investigate the effect of water content in different hydrophilic and hydrophobic ILs on the separation of phenolic compounds from LTCT. Furthermore, most studies in the literature mainly reported the effect of different IL structures on phenol extraction efficiency, which is not comprehensive.[3,4,23−27,34,35] There are also other separation indicators to consider, such as neutral oil entrainment, phenol distribution coefficient, and selectivity.

In this work, the phenol extraction capacity and selectivity of ILs with different water contents were calculated by COSMO-RS, and the solubility of oil in different IL−H_2O mixtures was also considered. The LTCT system is simplified with *m*-cresol as the representative phenolic compound and cumene and dodecane as model oil components. These ILs contain different types, chain lengths, and abilities to dissolve water, which can fully reflect the influence of water contents on the extraction phenol performance of ILs. After that, the effect of water on the extraction of phenols was analyzed by COSMO-RS. Furthermore, [C_2mim][Ac] was used as a representative IL, which was verified by experiments; the viscosity and ultraviolet−visible (UV−vis) spectra of [C_2mim][Ac] with different water contents were also measured.

2. RESULTS AND DISCUSSION

2.1. COSMO-RS Calculation Results. As previously reported, the structure and alkyl chain length of ILs can affect the affinity between ILs and water, and the effect of water content on the separation of phenolic compounds by different kinds of ILs is quite different.[30,31,34,36] The C_m^∞, S_{m1}^∞, and S_{m2}^∞ for *m*-cresol and the w_1 and w_2 for cumene and dodecane of the combinations of 15 cations and 8 anions with different water content were calculated by COSMO-RS, which contains the most representative cation and anion types as well as different imidazolium alkyl chain lengths.

First, eight [C_2mim]-based ILs combined with the anions of [Ac]$^-$, [Ala]$^-$, [H_2PO_4]$^-$, [DBP]$^-$, [TOS]$^-$, [$BuSO_4$]$^-$, [BF_4]$^-$, and [PF_6]$^-$ were selected, which range from strong hydrophilicity to strong hydrophobicity. The calculation results of the mass-based capacity, selectivity, and solubility of the IL−H_2O mixtures with different water contents are shown in Figures 1−3.

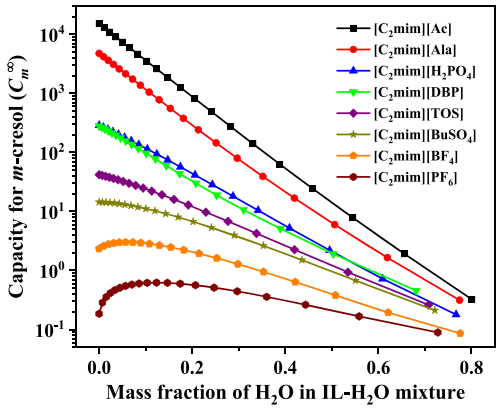

Figure 1. COSMO-RS calculated capacity for *m*-cresol (C_m^∞) of different [C_2mim]-based IL−H_2O mixtures with different mass fractions of water in the mixture.

As shown in Figure 1, when ILs contain strong hydrophilic anions ([Ac]$^-$, [Ala]$^-$, [H_2PO_4]$^-$, and [DBP]$^-$), the capacity for *m*-cresol decreases with the increase of water content in the IL−H_2O mixtures. For example, the capacity for *m*-cresol declines evidently from 15,076 of neat [C_2mim][Ac] to 7.82 of the [C_2mim][Ac]−H_2O mixture when the water content is 55 wt %. Gao et al. reported that the trend of capacity and extraction efficiency was highly consistent.[37] The addition of water could reduce the extraction efficiency for phenol of ChCl and [Et_4N][L-Ala], which verifies the accuracy of COSMO-RS.[30,31] For ILs with moderate hydrophilic anions ([TOS]$^-$ and [$BuSO_4$]$^-$), the capacity for *m*-cresol decreases slightly initially in a small range of water concentrations and then gradually decreases with the further increase of water concentration. Especially for [C_2mim][$BuSO_4$], the capacity for *m*-cresol is from 14.37 of neat IL to 14.08 of the IL−H_2O mixture with a water content of 2.4%. These facts indicate that

https://doi.org/10.1021/acsomega.1c04247
ACS Omega 2021, 6, 27368−27378

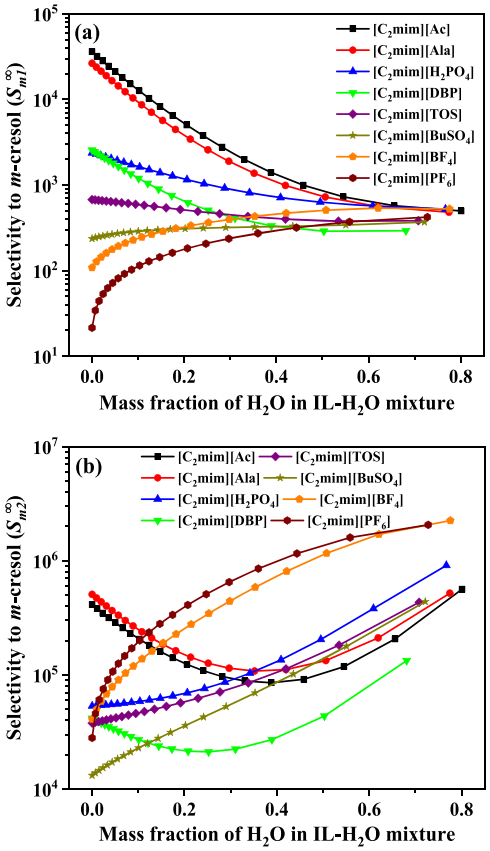

Figure 2. COSMO-RS calculated selectivity to *m*-cresol−cumene (a) and *m*-cresol−dodecane (b) of different [C_2mim]-based IL−H_2O mixtures with different mass fractions of water in the mixture.

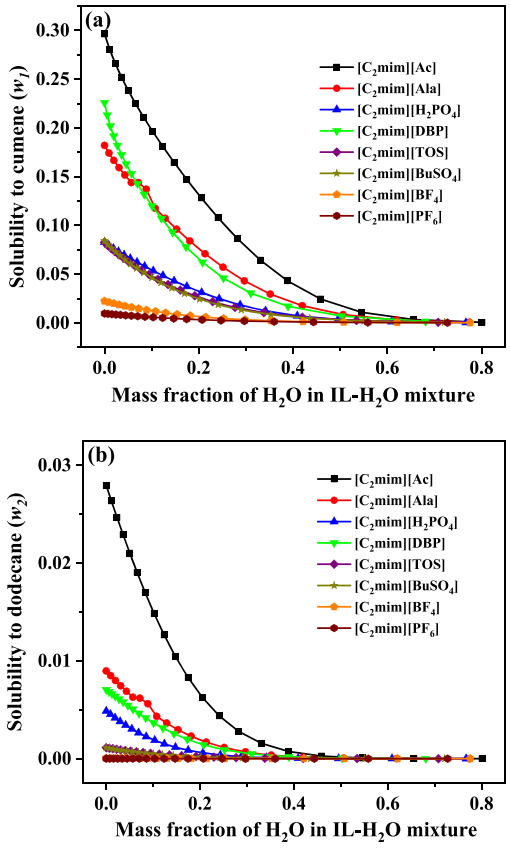

Figure 3. COSMO-RS calculated solubility to cumene (a) and dodecane (b) of different [C_2mim]-based IL−H_2O mixtures with different mass fractions of water in the mixture.

the presence of water in hydrophilic ILs will have adverse effects on the separation of phenolic compounds. On the contrary, the capacity for *m*-cresol of ILs containing hydrophobic anions ($[BF_4]^-$ and $[PF_6]^-$) increases when the water content is small and also decreases with a higher water content. For instance, the capacity obviously increases from 0.185 of neat [C_2mim][PF_6] to 0.617 when increasing the water content to 10 wt % in the [C_2mim][PF_6]−H_2O mixture and then decreases to 0.167 with the water content of 55 wt %. This indicates that the hydrophobic IL containing a small amount of water is acceptable, and it may be beneficial to the extraction and separation of phenolic compounds.

The effect of different water contents in the IL−H_2O mixture on the selectivity to *m*-cresol is also related to the hydrophilic ability of anions, and the influence of water content change on different separation systems is also dissimilar. In Figure 2a, for the *m*-cresol−cumene system, the selectivity to *m*-cresol decreases with the increase in water content from 0 to 70 wt % in the IL−H_2O mixtures with strong hydrophilic anions. The main reason is that the capacity for *m*-cresol of IL−H_2O mixtures decreases faster than cumene. Water content change has little effect on the selectivity to *m*-cresol of ILs containing moderate hydrophilic anions. For hydrophobic anions, the selectivity to *m*-cresol increases at first and then tends to be gently with the increase of water content. In Figure 2b, for the *m*-cresol−dodecane system, the selectivity to *m*-cresol is much higher than that of the *m*-cresol−cumene system; the results show that *m*-cresol is more easily separated from dodecane than cumene. For anions of $[Ac]^-$, $[Ala]^-$, and $[DBP]^-$, the selectivity to *m*-cresol decreases at first and then increases with the increase of water content in the IL−H_2O mixtures. For other anions, the selectivity of IL−H_2O mixtures increases quickly with the higher water content; it is indicated that the existence of water is beneficial to the separation of these ILs.

As can be seen in Figure 3, the solubility to cumene and dodecane in all IL−H_2O mixtures has a downward trend with higher water content, and the solubility of hydrophilic ILs is larger and decreases faster than that of hydrophobic ILs. Combining all the capacity, selectivity, and solubility, the effect of water on the separation performance is obviously different in IL−H_2O mixtures with hydrophilic and hydrophobic anions. Therefore, $[Ac]^-$ and $[PF_6]^-$ were selected as two representative anions to investigate the influence of water content on separation indexes with cations of different alkyl chain length, type, and functional group substitution.

The effect of different water content on the chain length of cationic alkyl with [$C_n$mim][Ac] and [$C_n$mim][PF_6] IL−H_2O mixtures (n = 2, 3, 4, 6, 8, and 12) is shown in Figures 4 and 5 and Figures S1−S3 (Supporting Information). In Figure 4a, the capacity for *m*-cresol of [$C_n$mim][Ac]−H_2O mixtures (n = 2, 3, 4, 6, 8, and 12) has an obvious downward trend from neat [$C_n$mim][Ac] to 30 wt % water content, and the decreasing tendency is faster with higher water content, while the length of alkyl side chain is shorter. At the same water content, the capacity decreases with the increase of alkyl side chain length. In Figure 4b, for [$C_n$mim][PF_6]−H_2O mixtures (n = 2, 3, 4, 6, 8, and 12), the capacity with different alkyl chain lengths has the same trend with rising water content; it increases within

https://doi.org/10.1021/acsomega.1c04247
ACS Omega 2021, 6, 27368−27378

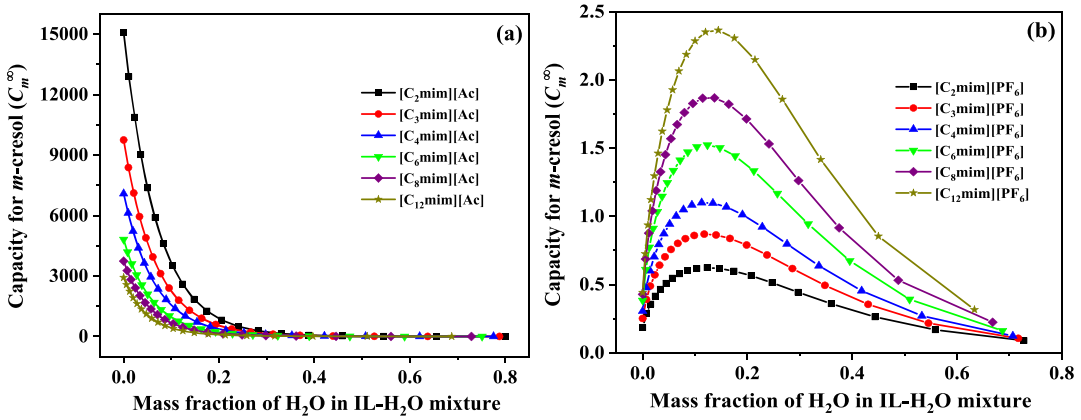

Figure 4. COSMO-RS calculated capacity for *m*-cresol (C_m^∞) of different [$C_n$mim][Ac] (a) and [$C_n$mim][PF_6] (b) IL−H_2O mixtures with different mass fractions of water in the mixture.

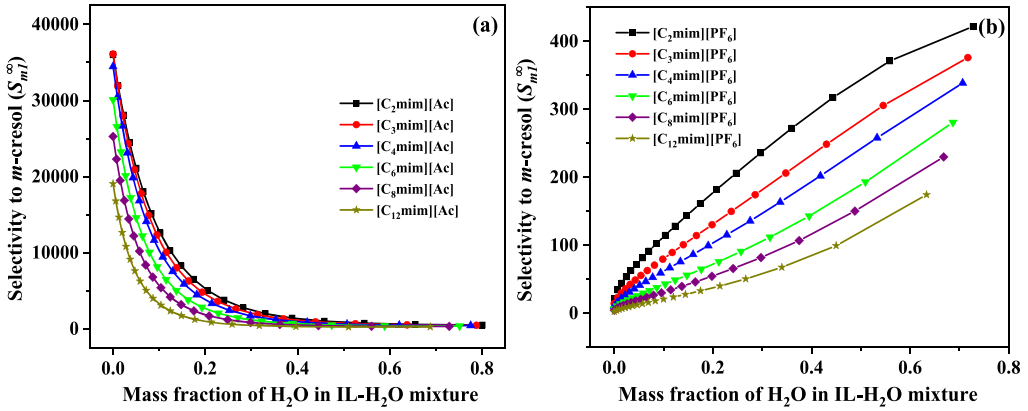

Figure 5. COSMO-RS calculated selectivity to *m*-cresol−cumene (S_{m1}^∞) of different [$C_n$mim][Ac] (a) and [$C_n$mim][PF_6] (b) IL−H_2O mixtures with different mass fractions of water in the mixture.

10% of water content and then decreases with further increase in water content. Unlike [$C_n$mim][Ac], the capacity increases with increasing alkyl side chain length for [$C_n$mim][PF_6]. The S_{m1}^∞ decreases with increasing water content for [$C_n$mim]-[Ac]−H_2O mixtures but increases for [$C_n$mim][PF_6]−H_2O mixtures (see Figure 5), and the effect of water content on S_{m2}^∞ is shown in Figure S1. Both S_{m1}^∞ and S_{m2}^∞ decrease with increasing alkyl chain length; it is indicated that the cation with a shorter alkyl side chain has a better separation effect. The solubility to cumene and dodecane of different [$C_n$mim]-based IL−H_2O mixtures decreases with growing water concentration (Figures S2 and S3, Supporting Information). The effect of water content on different cations with type and functional group substitution was also investigated in Figures S4 and S5. Along with the growth of water content, the capacity, selectivity, and solubility of IL−H_2O mixtures have a similar changing law with different cations for the same anion. In summary, the effect of water on the separation performance for phenolic compounds of IL−H_2O mixtures mainly depends on the structure of anions rather than cations in ILs by COSMO-RS calculation.

2.2. Molecular Interaction Analysis by COSMO-RS.

The separation performance of IL−H_2O mixtures can be analyzed from molecular interactions, which contain their σ-profile, σ-potential, and interaction energy between the solute and solvent. This analytical method has been successfully used to explain the separation mechanism of complex solvents.[38,39]

In the σ-profile, when σ exceeds ±0.0084 e·Å^{-2}, the molecule is supposed to have enough polarity to form hydrogen bonds. A molecule has hydrogen bond donor ability with σ < −0.0084 e·Å^{-2} and hydrogen bond acceptor ability with σ > 0.0084 e·Å^{-2}. The region of −0.0084 e·Å^{-2} < σ < 0.0084 e·Å^{-2} is named the nonpolar region.[40]

As shown in Figure 6, the σ-profile of *m*-cresol is majorly spread within the range of −0.021 e·Å^{-2} < σ < 0.016 e·Å^{-2}, and

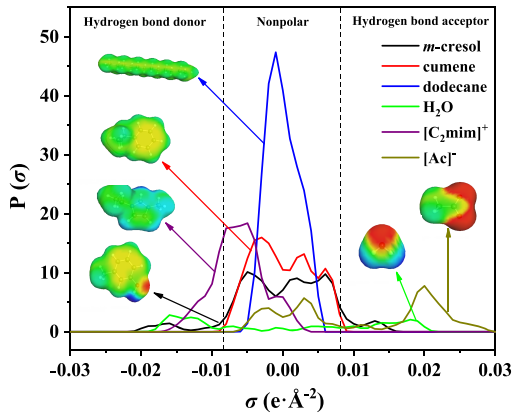

Figure 6. The σ-profiles of *m*-cresol, cumene, dodecane, H_2O, [C_2mim]$^+$, and [Ac]$^-$. Vertical dashed lines represent the threshold value for the hydrogen bonding interaction (σ_{hb} = ±0.0084 e·Å^{-2}).

https://doi.org/10.1021/acsomega.1c04247
ACS Omega 2021, 6, 27368−27378

m-cresol has two obvious peaks in the hydrogen bond donor region (σ = −0.016 e·Å^{-2}) and hydrogen bond acceptor region (σ = 0.013 e·Å^{-2}), indicating its intense ability to form hydrogen bond as a donor and an acceptor. This mainly depends on the hydrogen and oxygen atoms in the hydroxyl group. The σ-profile of the benzene ring in *m*-cresol and cumene is mainly concentrated in the nonpolar region. More notably, cumene also has a weak hydrogen bond donor and acceptor ability due to the distribution of σ-profile outside −0.0084 e·Å^{-2} < σ < 0.0084 e·Å^{-2}. For dodecane, the σ-profile is narrowly distributed within the range of −0.006 e·Å^{-2} < σ < 0.006 e·Å^{-2} and has an obvious peak at σ = 0 e·Å^{-2}. It is indicated that the polarity of dodecane is weaker than that of cumene. According to the theory of similar dissolve mutually, *m*-cresol is more easily dissolved in IL−H_2O mixtures with strong polarity and more easily separated from dodecane than cumene.

For the IL−H_2O mixture, with [C_2mim][Ac] taken as an example, [Ac]$^-$ has a strong peak at σ = 0.02 e·Å^{-2}, suggesting its strong hydrogen acceptor donor ability. [C_2mim]$^+$ is less distributed in the hydrogen bond donor region. It is suggested that it is easier for [Ac]$^-$ than [C_2mim]$^+$ to form a hydrogen bond with *m*-cresol. Both [C_2mim]$^+$ and [Ac]$^-$ present strong peaks in the negative nonpolar region, indicating that [C_2mim][Ac] can also dissolve a certain amount of cumene and dodecane. Compared with *m*-cresol, water as a solvent has a wider distribution in the hydrogen bond donor and acceptor region, which can interact with [C_2mim][Ac] to form a stronger hydrogen bond than that between *m*-cresol and [C_2mim][Ac]. The competitive relationship between water and *m*-cresol leads to the decrease of capacity for *m*-cresol with higher water content (see Figure 1). Furthermore, the σ-profile of H_2O has almost no distribution in the nonpolar region, which causes decreasing solubility for cumene and dodecane with increasing water content (see Figure 3).

The σ-profiles of different anions and cations are shown in Figure S6 (Supporting Information). The hydrophilic ability of ILs enhances with the increasing hydrogen bond acceptor ability of anions. The IL−H_2O mixture with a strong hydrogen bond acceptor ability anion has better separation performance for *m*-cresol, which can also be explained by the HB-acc3 of anions (see Table S4). For example, the HB-acc3 of [Ac]$^-$ is 38.9278, which is the largest among all anions, and the IL−H_2O mixture containing [Ac]$^-$ has the highest capacity and selectivity for *m*-cresol. The σ-profiles of different cations are similar, which lead to the same effect of water content on IL−H_2O mixtures with different cations.

The chemical potential of a surface segment (also called σ-potential) is calculated from statistical thermodynamics with molecular interactions according to the calculated σ-profile.[41] The whole σ-potential range is also divided into three regions by the hydrogen bond threshold (σ_{hb} = ± 0.0084 e·Å^{-2}). The nonpolar region (−0.0084 e·Å^{-2} < σ < 0.0084 e·Å^{-2}) represents nonpolar interaction. Unlike the σ-profile, the electronic basicity region (σ < −0.0084 e·Å^{-2}) and the electronic acidity region (σ > 0.0084 e·Å^{-2}) show hydrogen bond acceptor and hydrogen bond donor intensity, respectively.[42] In each region of the σ-potential, a solvent has a stronger molecular interaction with other compounds while having a higher negative value of $\mu(\sigma)$. On the contrary, a higher positive value represents a higher repulsive force. The σ-potentials of *m*-cresol, cumene, dodecane, H_2O, and [C_2mim][Ac] are shown in Figure 7.

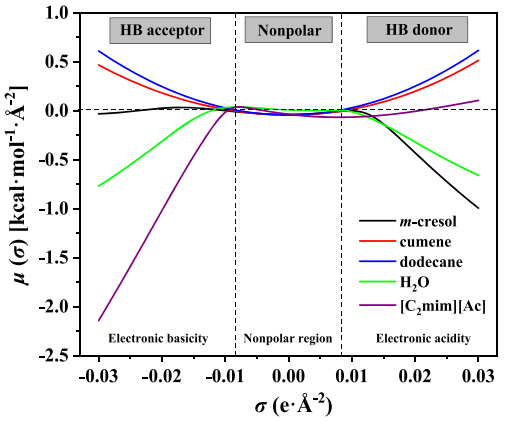

Figure 7. The σ-potentials of *m*-cresol, cumene, dodecane, H_2O, and [C_2mim][Ac].

The σ-potentials of *m*-cresol and [C_2mim][Ac] present a negative value in the electronic acidity and basicity region, respectively. It is indicated that a strong hydrogen bond interaction can be formed between [C_2mim][Ac] and *m*-cresol. The σ-potentials of cumene, dodecane, and [C_2mim]-[Ac] all have negative values in the nonpolar region, suggesting their nonpolar interaction. H_2O has almost no negative value in the nonpolar region, which has a higher negative value in both the electronic acidity and basicity regions. This fully proves that H_2O has a strong hydrogen bond acceptor and donor ability at the same time. The σ-potentials for [C_2mim][Ac]−H_2O mixtures with different water contents are plotted in Figure 8.

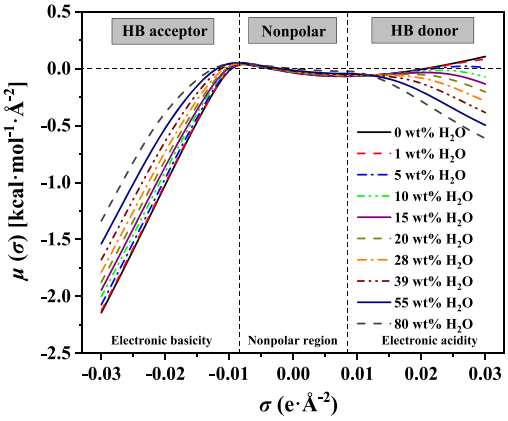

Figure 8. The σ-potentials of [C_2mim][Ac]−H_2O mixtures with different water contents.

[C_2mim][Ac]−H_2O mixtures have lower negative values in the electronic basicity region and nonpolar region but higher negative values in the electronic acidity region with increasing water content. In the process of forming a hydrogen bond, *m*-cresol and the [C_2mim][Ac]−H_2O mixture act as the hydrogen bond donor and acceptor, respectively. The strength of the hydrogen bond interaction between the [C_2mim][Ac]−H_2O mixture and *m*-cresol decreases with higher water content due to the decreasing hydrogen bond acceptor ability of the [C_2mim][Ac]−H_2O mixture. The strength of the nonpolar interaction between the [C_2mim][Ac]−H_2O mixture and cumene as well as dodecane also decreases with the increase of water content. The σ-potential of ILs containing different

https://doi.org/10.1021/acsomega.1c04247
ACS Omega 2021, 6, 27368−27378

anions varies widely especially in the electronic basicity region. On the contrary, the σ-potential distribution containing different cations is similar (see Figure S7, Supporting Information). These are consistent with the results of the calculated capacity for *m*-cresol as well as solubility for cumene and dodecane (see Figures 1−3).

In the COSMO-RS theory, the intermolecular interaction energy included the misfit energy, the hydrogen bond (HB) energy, and the van der Waals (vdW) energy. The significance and calculation details can be found in the previous literature.[43,44] To further investigate the effect of water content in IL−H_2O mixtures on the separation of *m*-cresol, three types of the intermolecular interaction energies between *m*-cresol and the [C_2mim][Ac]−H_2O mixture with different water contents are calculated in Figure 9.

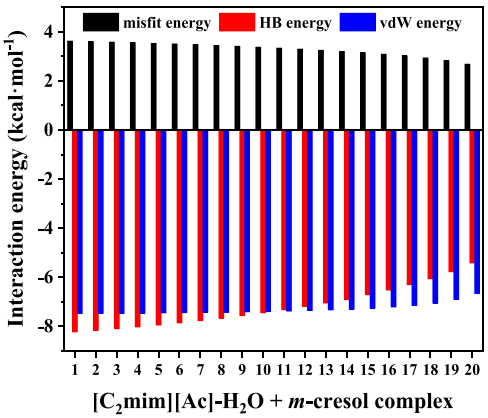

Figure 9. Intermolecular interaction energies of *m*-cresol with the [C_2mim][Ac]−H_2O mixture calculated by COSMO-RS at 25 °C (abscissas 1−20 represent a gradually increasing water content from 0 to 80 wt %).

The HB energy and vdW energy have lower negative values, while the misfit energy shows lower positive values, between *m*-cresol and the [C_2mim][Ac]−H_2O mixture with increasing water content in the [C_2mim][Ac]−H_2O mixture. Compared with the misfit and vdW energy, the decreasing trend of HB energy is more obvious. For instance, the misfit, HB, and vdW energy for neat [C_2mim][Ac] is 3.623, −8.227, and −7.480 kcal·mol^{-1}, respectively. The energy declines to 2.683, −5.415, and −6.663 kcal·mol^{-1} when the water content is 80 wt %, respectively. The hydrogen bond interaction plays a leading role in the extraction process, and the capacity for *m*-cresol of the [C_2mim][Ac]−H_2O mixture decreases from 15,076 to 0.323 with decreasing HB energy from −8.227 to −5.415 kcal·mol^{-1}.[45] The same trend for the misfit and vdW energy change between cumene, dodecane, and the [C_2mim][Ac]−H_2O mixture is shown in Figure S8. The HB interactions can be neglected due to the strong nonpolarity of cumene and dodecane. The misfit energy and vdW energy are used to measure the electrostatic interaction and vdW interaction, respectively. Lower vdW energy and higher misfit energy can reduce the solubility of oil in the IL−H_2O mixture. For instance, the vdW energies between the [C_2mim][Ac]−H_2O mixture and cumene gradually decrease from −9.012 to −8.868 kcal·mol^{-1}, and the misfit energies increase from 3.395 to 3.496 kcal·mol^{-1}; meanwhile, and the corresponding solubilities of cumene in [C_2mim][Ac]−H_2O decrease from 0.296 to 0.108. Compared with the electrostatic interaction, the vdW interaction plays a major role in oil in IL−H_2O mixture systems. This was confirmed by the lower solubility of cumene and dodecane in the IL−H_2O mixture with higher water content.

In conclusion, the effect of different water contents for IL−H_2O mixtures on separation performance indexes such as capacity and solubility can be reasonably explained by the molecular interactions.

2.3. Experimentally Determined Effect of Water on Phenol Separation of IL−H_2O Mixtures. Based on the results of the COSMO-RS calculation, ILs have a higher separation performance for phenols with the increase of hydrophilicity. This has been confirmed on the phenol separation performance of ILs with hydrophilic and hydrophobic anions ([Ac]$^-$, [Cl]$^-$, [Br]$^-$, [BF_4]$^-$, and [PF_6]$^-$).[23,26] Therefore, the easily obtained strong hydrophilic [C_2mim][Ac] was selected as the representative to research the effect of water content on the extraction of phenolic compounds from model oil.

In our previous research, the experimental conditions of extracting *m*-cresol from model oil by [C_2mim][Ac] have been optimized.[26] The effect of water content on the *m*-cresol separation performance of the [C_2mim][Ac]−H_2O mixture was researched under optimal conditions (the stirring time, settling time, temperature, and mass ratio of [C_2mim][Ac]/model oil were 30 min, 30 min, 25 °C, and 0.5:1, respectively).

As seen in Figure 10a, the *m*-cresol extraction efficiency decreases from 99.8% for neat [C_2mim][Ac] to 95.9% for the [C_2mim][Ac]−H_2O mixture with the water content of 50.1%. It is consistent with the decreasing capacity for *m*-cresol with increasing water content in the [C_2mim][Ac]−H_2O mixture. The entrainment of cumene increases from 21.4 to 27.9% when the water content in [C_2mim][Ac] increases from 0.1 to 7.7 wt %. Then, a decreasing cumene entrainment is discovered with further increasing water content to 19.9 wt %, and it continued to rise as the water content increased. The variation of dodecane entrainment is the same as cumene, and the amount of dodecane entrainment is less than cumene. To further comprehend the phase equilibrium relationship between the IL−H_2O mixture + *m*-cresol + cumene + dodecane in the extraction process, the liquid−liquid phase equilibrium data and pseudo ternary phase diagram of this system are shown in Table S5 and Figure S9, respectively. The pseudo ternary phase diagram indicates that *m*-cresol has a higher affinity toward [C_2mim][Ac]−H_2O than cumene and dodecane. With the increase of water content in [C_2mim][Ac], the content of *m*-cresol is increased gradually in the upper phase; the variation of cumene and dodecane content in the lower phase is in good agreement with the variation of cumene and dodecane entrainment in the extraction process. A certain amount of cumene and dodecane could be also dissolved in the [C_2mim][Ac]−H_2O phase. Because the polarity of water is weaker than that of [C_2mim][Ac] (see Figures 6 and 7), the polarity of the [C_2mim][Ac]−H_2O mixture decreases with less water content, resulting in the increase of neutral oil entrainment. The solubility of neutral oil in water is very small, and the neutral oil entrainment in the [C_2mim][Ac]−H_2O phase decreases with the further increase in water content.

It is worth noting that the three-phase system was formed and led to a more complex effect on the *m*-cresol separation process when the water content increased to 20.0 wt %. This is mainly because water and *m*-cresol are immiscible. When the

https://doi.org/10.1021/acsomega.1c04247
ACS Omega 2021, 6, 27368−27378

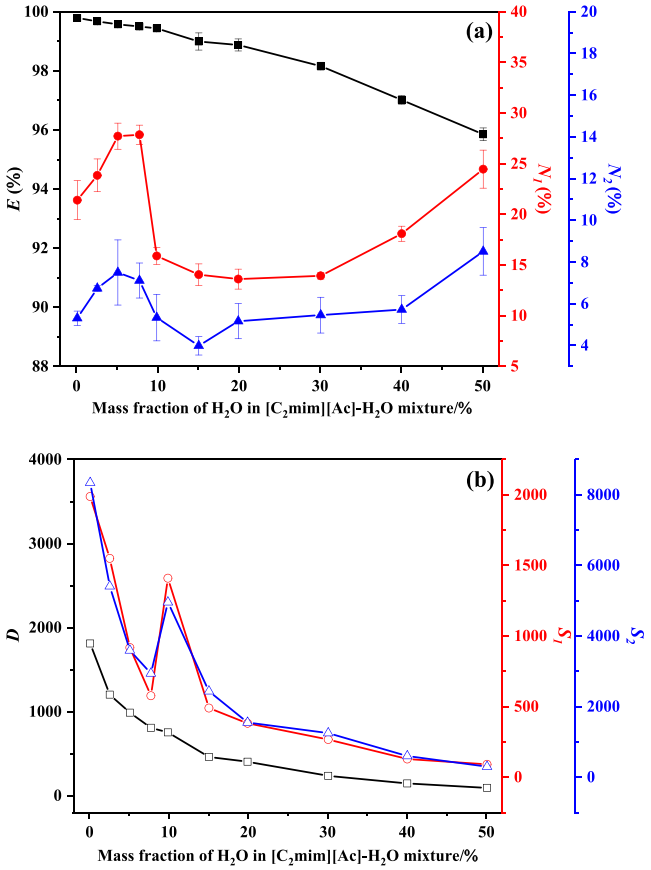

Figure 10. Experimentally determined effect of water content in the $[C_2mim][Ac]-H_2O$ mixture on phenol separation performance of (a) *m*-cresol extraction efficiency (E) and entrainment of cumene (N_1) and dodecane (N_2) and (b) *m*-cresol distribution coefficient (D) and selectivity to cumene (S_1) and dodecane (S_2).

water content of $[C_2mim][Ac]$ is high, *m*-cresol cannot be completely dissolved in $[C_2mim][Ac]-H_2O$, and then part of the mixture of *m*-cresol and water could precipitate as the third phase. The broad absorption peak of the $[C_2mim][Ac]-H_2O$ mixture also shows obvious shifts leftward with water content over 20% in the UV−vis spectra (Figure S10, Supporting Information), indicating the leading role of water in the IL−H_2O mixtures at this moment.

To further evaluate the separation effect, the effect of water content in the $[C_2mim][Ac]-H_2O$ mixture on the distribution coefficient and selectivity of *m*-cresol is shown in Figure 10b. The *m*-cresol distribution coefficient decreases from 1810.8 to 92.9 with water content from neat $[C_2mim][Ac]$ to 50.1%, which has the same trend as the extraction efficiency. The selectivity of *m*-cresol to both cumene and dodecane decreases with increasing water content, except for the mutation when the water content is 10%. This is because the entrainment of cumene and dodecane in the IL−H_2O phase is less, and the extraction efficiency of *m*-cresol is still higher at 10% moisture content. In conclusion, the presence of water has an adverse effect on the separation of phenolic compounds for hydrophilic ILs.

In addition, viscosity is an important physical property of ILs. ILs with high viscosity are not conducive to mass transfer and cause high energy consumption. The viscosity change of the $[C_2mim][Ac]-H_2O$ mixture with different water contents is shown in Figure 11.

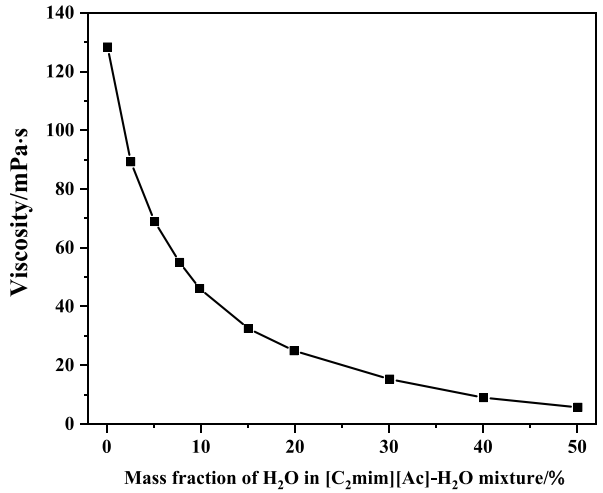

Figure 11. Viscosity of the $[C_2mim][Ac]-H_2O$ mixture with different water contents.

The viscosity of $[C_2mim][Ac]$ gradually decreases with increasing water content from neat $[C_2mim][Ac]$ to 50.1%. The experimental and previous literature viscosities of the $[C_2mim][Ac]-H_2O$ mixture are compared in Figure S11 (Supporting Information).[46,47] It is noteworthy that the viscosity is only 128.3 mPa·s of neat $[C_2mim][Ac]$, which is much smaller than that of DILs and ILs containing halogen anions.[25,48,49] Combined with the separation performance, ILs should be dried to remove water as much as possible before use so as to ensure the separation effect of phenols and avoid the production of phenol containing wastewater.

3. CONCLUSIONS

The effect of water in ILs on the separation performance of phenols was studied by COSMO-RS calculation and experiments. The results of COSMO-RS calculation show that water has a great influence on the phenol separation performance with different anions in ILs, while it has little effect on different cations. The ILs containing hydrophilic anions demonstrate a negative effect on the phenol separation with increasing water content and show a positive effect with hydrophobic anions in a small amount of water content. The phenol separation effect of hydrophilic ILs is much better than that of hydrophobic ILs. $[C_2mim][Ac]$ with strong hydrophilicity is used as a representative IL, and the molecular interaction analysis results indicate that the hydrogen bond interaction is the main interaction between $[C_2mim][Ac]$ and *m*-cresol. The competition between water and *m*-cresol leads to the decrease of the hydrogen bond interaction energy between the $[C_2mim][Ac]-H_2O$ mixture and *m*-cresol with increasing water content. The experimental results show that the presence of water can reduce the separation performance of $[C_2mim][Ac]$ for *m*-cresol. ILs should be dried and dehydrated before using to ensure the separation effect of phenols from LTCT.

4. SIMULATION AND EXPERIMENTAL DESCRIPTION

4.1. COSMO-RS Calculation. The COSMO-RS model can directly and quickly predict the thermodynamic properties of liquids without relying on experimental data. The relevant calculation details of COSMO-RS model have been given in the previous literature.[40,41,50] The calculation process is mainly divided into two steps. First, the screening charge density (also

https://doi.org/10.1021/acsomega.1c04247
ACS Omega 2021, 6, 27368−27378

called σ-profile) of the compounds should be obtained by quantum chemical calculation, and this process is usually time-consuming. The good news is that the current COSMO database contains the σ-profiles of common organic compounds and hundreds of cations and anions of ILs. In this work, all the σ-profiles of the representative compounds from LTCT, involved cations and anions of ILs were selected from the database of the COSMOthermX software (Version 18.0.0). The COSMO-RS calculations were carried out with the BP_TZVP_18 parameterization. The information of cations, anions, and representative compounds is tabulated in Tables S1−S3 (Supporting Information).

Then, the thermodynamic properties can be predicted by calculating the chemical potential of representative compound i in different solvents with the COSMO-RS model. For example, the activity coefficient at an arbitrary concentration can be calculated by eq 1:

$$\ln(\gamma_i) = (\mu_i^{sol} - \mu_i^{com})/RT \quad (1)$$

where μ_i^{sol} and μ_i^{com} represent the chemical potential of the compound i in the solvent and in the pure compound, respectively. The mole-based capacity (C^{∞}) and selectivity (S^{∞}) of the solvent can be obtained by calculating the activity coefficient at infinite dilution through eqs 2 and 3. These two indexes are extensively used to evaluate the separation effect of a solvent in the literature.[37,51,52]

$$C^{\infty} = (1/\gamma_i^{\infty})^{sol} \quad (2)$$

$$S^{\infty} = (\gamma_j^{\infty}/\gamma_i^{\infty})^{sol} \quad (3)$$

where γ_i^{∞} and γ_j^{∞} represent the infinite dilution activity coefficient of solute i and diluent j in the solvent phase, respectively. Song et al. further reported that some solvents showed only better mole-based, but not mass-based, separation performance due to the larger molecular weight.[53,54] To solve this problem, the mass-based capacity (C_m^{∞}) and selectivity (S_{m1}^{∞} and S_{m2}^{∞}) of the IL−H_2O mixtures are calculated using eqs 4−6:

$$C_m^{\infty} = (1/\gamma_{m-cresol}^{\infty,LAB}) \times (MW_{m-cresol}/MW_{IL\text{-}H_2O}) \quad (4)$$

$$S_{m1}^{\infty} = (\gamma_{cumene}^{\infty,LAB}/\gamma_{m-cresol}^{\infty,LAB}) \times (MW_{m-cresol}/MW_{cumene}) \quad (5)$$

$$S_{m2}^{\infty} = (\gamma_{dodecane}^{\infty,LAB}/\gamma_{m-cresol}^{\infty,LAB}) \times (MW_{m-cresol}/MW_{dodecane}) \quad (6)$$

where C_m^{∞} refers to the mass-based capacity of IL−H_2O mixtures to m-cresol and S_{m1}^{∞} and S_{m2}^{∞} refer to the mass-based selectivity of IL−H_2O mixtures to m-cresol against cumene and dodecane, respectively. $MW_{m-cresol}$, MW_{IL-H_2O}, MW_{cumene}, and $MW_{dodecane}$ refer to the molecular weight of m-cresol, IL−H_2O mixtures, cumene, and dodecane, respectively. Significantly, the electro-neutral approach is carried out in this work to describe IL−H_2O mixtures in COSMO-RS. Therefore, it is necessary to correct the infinite dilution activity coefficient calculated by COSMO-RS. The correction method is the same as deep eutectic solvents (DESs) in the literature.[55,56] $\gamma_{m-cresol}^{\infty,LAB}$, $\gamma_{cumene}^{\infty,LAB}$, and $\gamma_{dodecane}^{\infty,LAB}$ refer to the modified infinite dilution activity coefficients of m-cresol, cumene, and dodecane.

To investigate the effect of different water contents in IL−H_2O mixtures on neutral oil entrainment in the extraction process, the mole-based solubility of oil in IL−H_2O mixtures solvent is calculated by eq 7:

$$\log_{10}(x_i) = (\mu_i^{oil} - \mu_i^{sol} - \Delta G_{i,fusion})/RT\ln 10 \quad (7)$$

where $\Delta G_{i,\,fusion}$ is the Gibbs free energy of fusion. All of the ILs−H_2O mixture solvents involved in this work are assumed to be liquids at room temperature, so their $\Delta G_{i,\,fusion}$ can be set to zero. The solubility (x_i) calculated by eq 7 is a zero-order approximation; x_i can be improved by iterative calculation using eq 8:

$$\log_{10}(x_i^{(n+1)}) = (\mu_i^{oil} - \mu_i^{sol(n)} - \Delta G_{i,fusion})/RT\ln 10 \quad (8)$$

Similarly, it is necessary to modify the solubility calculated by COSMO-RS in the same way as the infinite dilution activity coefficient. The mass-based solubility (w_1 and w_2) can be calculated from the modified mole-based solubility (x_1^{LAB} and x_2^{LAB}) by eqs 9 and 10:

$$w_1 = (x_1^{LAB} \times MW_{cumene})/[(1 - x_1^{LAB}) \times MW_{IL\text{-}H_2O}] \quad (9)$$

$$w_2 = (x_2^{LAB} \times MW_{dodecane})/[(1 - x_2^{LAB}) \times MW_{IL\text{-}H_2O}] \quad (10)$$

where w_1 and w_2 refer to the mass-based solubility of cumene and dodecane in the IL−H_2O mixture solvent, respectively. The accuracy of COSMO-RS calculated infinite dilution activity coefficient and solubility has been verified in the previous literature.[26,43,51,52,57−59]

4.2. Experimental Section. The IL [C_2mim][Ac], m-cresol, cumene, dodecane, and o-nitrotoluene were purchased from Shanghai Macklin Biochemical Co., Ltd., with a purity above 99.0 wt %. Absolute alcohol (≥99.5 wt %) was purchased from Modern Oriental (Beijing) Technology Development Co., Ltd. Except for [C_2mim][Ac], all the chemicals in the experiments were used without further purification. Before use, [C_2mim][Ac] was dried for 60 h at 80 °C under reduced pressure to remove the moisture as much as possible. After the removal of water, the water content in [C_2mim][Ac] was not more than 1000 mg·kg^{-1} with a 870 KF Titrino plus Karl Fischer Moisture Titrator (Switzerland).

Twenty grams of dried [C_2mim][Ac] was added to a 50 mL screw-capped glass bottle, and a specific amount of water was added gravimetrically to obtain the [C_2mim][Ac]−H_2O mixture solvents with a water content of 2.5, 5.0, 7.5, 10.0, 15.0, 20.0, 30.0, 40.0, and 50.0 wt %, respectively. The viscosities of [C_2mim][Ac]−H_2O mixture solvents with different water contents were measured by a viscometer with a Brookfield DVESLVTJ0 within ±0.5% (USA) at 25 °C with a DC0506N thermostatic bath within ±0.1 °C (China). The absorbance of these solvents was also determined by a UV-1100 Spectrophotometer with Mapapa (China).

In the extraction experiments, the model oil consisted of 30 wt % m-cresol, 50 wt % cumene, and 20 wt % dodecane. Ten grams of the model oil was first added to a 25 mL screw-capped glass bottle, and then 5 g of the prepared [C_2mim]-[Ac]−H_2O mixture solvent was added into this bottle. After sealing, the mixture was stirred with a magnetic stirrer for 30 min at 25 °C. The speed of revolution was set to 600 rpm. After stirring, the mixture was stood for 1 h; the liquid−liquid stratification could be clearly observed. During the experiments, the mixture temperature was controlled by an HWCL-3 constant temperature water bath within ±0.1 °C (China). All weighing was performed with a AE224C analytical balance within ±0.0001 g (China).

https://doi.org/10.1021/acsomega.1c04247
ACS Omega 2021, 6, 27368−27378

After that, the upper dephenol oil phase was carefully removed from the lower IL−H_2O mixture phase by a separating funnel, and the mass of the upper phase was measured carefully. The upper phase oil (0.5 mL) and *o*-nitrotoluene (0.5 mL, internal standard) were added into a 10 mL screw-capped glass bottle with a pipette gun, and the mass of the transferred liquids was accurately weighed. The mixture was diluted five times with anhydrous ethanol to obtain the sample. The composition of sample was analyzed by a GC-SP3420 gas chromatograph (China) equipped with a flame ionization detector (FID) and a KB-WAX (50 m × 0.25 mm × 0.25 μm) column. The column temperature program of the GC was started at 80 °C, settled for 2 min, increased at a rate of 3 °C·min^{-1} until the temperature reached 120 °C, settled for 1 min, increased at a rate of 10 °C·min^{-1} until the temperature reached 200 °C, and settled for 15 min. The total analysis time was 39.33 min. The temperature of the injection port and FID was set at 230 °C. The injection volume of the sample was 0.6 μL. The extraction separation indexes such as *m*-cresol extraction efficiency (E (%)), distribution coefficient (D), selectivity of *m*-cresol−cumene (S_1) and *m*-cresol−dodecane (S_2), and entrainment of cumene (N_1 (%)) and dodecane (N_2 (%)) were calculated according to eqs 11−16:

$$E(\%) = (m_{m-\text{cresol}} - w_{m-\text{cresol}} \cdot m_U)/m_{m-\text{cresol}} \times 100\% \quad (11)$$

$$D = w'_{m-\text{cresol}}/w_{m-\text{cresol}} \quad (12)$$

$$S_1 = (w'_{m-\text{cresol}}/w_{m-\text{cresol}})/(w'_{\text{cumene}}/w_{\text{cumene}}) \quad (13)$$

$$S_2 = (w'_{m-\text{cresol}}/w_{m-\text{cresol}})/(w'_{\text{dodecane}}/w_{\text{dodecane}}) \quad (14)$$

$$N_1(\%) = (m_{\text{cumene}} - w_{\text{cumene}} \cdot m_U)/m_{\text{cumene}} \times 100\% \quad (15)$$

$$N_2(\%) = (m_{\text{dodecane}} - w_{\text{dodecane}} \cdot m_U)/m_{\text{dodecane}} \times 100\% \quad (16)$$

where $m_{m-\text{cresol}}$, m_{cumene}, m_{dodecane}, and m_U refer to the mass of *m*-cresol, cumene, and dodecane in the model oil and upper phase oil, respectively. $w_{m-\text{cresol}}$, w_{cumene}, w_{dodecane}, $w'_{m-\text{cresol}}$, w'_{cumene}, and w'_{dodecane} refer to the mass fraction of *m*-cresol, cumene, and dodecane in the upper phase and lower phase, respectively.

■ ASSOCIATED CONTENT

Supporting Information

The Supporting Information is available free of charge at https://pubs.acs.org/doi/10.1021/acsomega.1c04247.

Details of chemical structures; capacity, selectivity, and solubility of different ILs; HB-acc3 and σ-profiles of the anions and cations; σ-potentials of different ILs; intermolecular interaction energies of cumene and dodecane with [C_2mim][Ac]−H_2O; LLE data and pseudo ternary system of the {([C_2mim][Ac]−H_2O) + *m*-cresol + (cumene + dodecane)} system; UV−vis spectra of different compounds; and comparison of [C_2mim][Ac]−H_2O viscosity with the previous literature (PDF)

■ AUTHOR INFORMATION

Corresponding Author

Xianglan Zhang − *School of Chemical and Environmental Engineering, China University of Mining and Technology (Beijing), Beijing 100083, China;* orcid.org/0000-0001-5435-1285; Email: zhxl@cumtb.edu.cn

Authors

Qian Liu − *School of Chemical and Environmental Engineering, China University of Mining and Technology (Beijing), Beijing 100083, China*

Jing Bi − *School of Chemical and Environmental Engineering, China University of Mining and Technology (Beijing), Beijing 100083, China*

Complete contact information is available at: https://pubs.acs.org/10.1021/acsomega.1c04247

Notes

The authors declare no competing financial interest.

■ ACKNOWLEDGMENTS

The authors thank the financial support provided by the National Key Research and Development Program of China (2016YFB0600305).

■ REFERENCES

(1) Yi, L.; Feng, J.; Li, W.; Luo, Z. High-performance separation of phenolic compounds from coal-based liquid oil by deep eutectic solvents. *ACS Sustainable Chem. Eng.* **2019**, *7*, 7777−7783.

(2) Gai, H.; Qiao, L.; Zhong, C.; Zhang, X.; Xiao, M.; Song, H. A solvent based separation method for phenolic compounds from low-temperature coal tar. *J. Cleaner Prod.* **2019**, *223*, 1−11.

(3) Jiao, T.; Gong, M.; Zhuang, X.; Li, C.; Zhang, S. A new separation method for phenolic compounds from low-temperature coal tar with urea by complex formation. *J. Ind. Eng. Chem.* **2015**, *29*, 344−348.

(4) Jiao, T.; Li, C.; Zhuang, X.; Cao, S.; Chen, H.; Zhang, S. The new liquid−liquid extraction method for separation of phenolic compounds from coal tar. *Chem. Eng. J.* **2015**, *266*, 148−155.

(5) Sun, Q. J.; Ma, X. X.; Sun, C. S.; Xu, J. L. Study on the phenolic compounds extraction and separation in mid low-temperature coal tar of northern Shanxi. *Appl. Chem. Ind.* **2013**, *42*, 713−716.

(6) Lin, Z.; Hou, Y.; Ren, S.; Ji, Y.; Yao, C.; Niu, M.; Wu, W. Phase equilibria of phenol + toluene + quaternary ammonium salts for the separation of phenols from oil with forming deep eutectic solvents. *Fluid Phase Equilib.* **2016**, *429*, 67−75.

(7) Yao, C.; Hou, Y.; Ren, S.; Ji, Y.; Wu, W. Ternary phase behavior of phenol + toluene + zwitterionic alkaloids for separating phenols from oil mixtures via forming deep eutectic solvents. *Fluid Phase Equilib.* **2017**, *448*, 116−122.

(8) Li, G.; Xie, Q.; Liu, Q.; Liu, J.; Wan, C.; Liang, D.; Zhang, H. Separation of phenolic compounds from oil mixtures by betaine-based deep eutectic solvents. *Asia-Pac. J. Chem. Eng.* **2020**, *15*, No. e2515.

(9) Yao, C. F.; Hou, Y. C.; Ren, S. H.; Ji, Y. A.; Wu, W. Z.; Liu, H. Efficient separation of phenolic compounds from model oils by dual-functionalized ionic liquids. *Chem. Eng. Process.* **2018**, *128*, 216−222.

(10) Li, A.; Xu, X.; Zhang, L.; Gao, J.; Xu, D.; Wang, Y. Separation of cresol from coal tar by imidazolium-based ionic liquid [Emim]-[SCN]: Interaction exploration and extraction experiment. *Fuel* **2020**, *264*, 116908.

(11) Schobert, H. H.; Song, C. Chemicals and materials from coal in the 21st century. *Fuel* **2002**, *81*, 15−32.

(12) Gai, H. J.; Qiao, L.; Zhong, C. Y.; Zhang, X. W.; Xiao, M.; Song, H. B. Designing ionic liquids with dual lewis basic sites to efficiently separate phenolic compounds from low-temperature coal tar. *ACS Sustainable Chem. Eng.* **2018**, *6*, 10841−10850.

(13) Meng, H.; Ge, C. T.; Ren, N. N.; Ma, W. Y.; Lu, Y. Z.; Li, C. X. Complex extraction of phenol and cresol from model coal tar with polyols, ethanol amines, and ionic liquids thereof. *Ind. Eng. Chem. Res.* **2014**, *53*, 355−362.

(14) Jiao, T. T.; Wang, H. Y.; Dai, F.; Li, C. S.; Zhang, S. J. Thermodynamics study on the separation process of cresols from hexane via deep eutectic solvent formation. *Ind. Eng. Chem. Res.* **2016**, *55*, 8848−8857.
(15) Liu, X. K.; Zhang, X. L. Solvent screening and liquid-liquid measurement for extraction of phenols from aromatic hydrocarbon mixtures. *J. Chem. Thermodyn.* **2019**, *129*, 12−21.
(16) Kang, X. C.; Sun, X. F.; Han, B. X. Synthesis of functional nanomaterials in ionic liquids. *Adv. Mater.* **2016**, *28*, 253−266.
(17) Yang, A.; Zou, H. C.; Chien, I. L.; Wang, D.; Wei, S. A.; Ren, J. Z.; Shen, W. F. Optimal design and effective control of triple-column extractive distillation for separating ethyl acetate/ethanol/water with multiazeotrope. *Ind. Eng. Chem. Res.* **2019**, *58*, 7265−7283.
(18) Sun, S. R.; Chun, W.; Yang, A.; Shen, W. F.; Cui, P. Z.; Ren, J. Z. The separation of ternary azeotropic mixture: Thermodynamic insight and improved multi-objective optimization. *Energy* **2020**, *206*, 118117.
(19) Yang, A.; Su, Y.; Shi, T.; Ren, J. Z.; Shen, W. F.; Zhou, T. Energy-efficient recovery of tetrahydrofuran and ethyl acetate by triple-column extractive distillation: entrainer design and process optimization. *Front. Chem. Sci. Eng.* **2021**, DOI: 10.1007/s11705-021-2044-z.
(20) Mikkola, J. P.; Virtanen, P.; Karhu, H.; Salmia, T.; Murzin, D. Supported ionic liquids catalysts for fine chemicals: citral hydrogenation. *Green Chem.* **2006**, *8*, 197−205.
(21) Li, Y.; Zhang, X. P.; Lai, S. Y.; Dong, H. F.; Chen, X. L.; Wang, X. L.; Nie, Y.; Sheng, Y.; Zhang, S. J. Ionic liquids to extract valuable components from direct coal liquefaction residues. *Fuel* **2012**, *94*, 617−619.
(22) Sun, D. Z.; Feng, H. S.; Feng, X.; Li, W. X.; Zhang, Z. G. Feasibility of ionic liquid as extractant for bio-butanol extraction: experiment and simulation. *Sep. Purif. Technol.* **2019**, *215*, 287−298.
(23) Hou, Y. C.; Ren, Y. H.; Peng, W.; Ren, S. H.; Wu, W. Z. Separation of phenols from oil using imidazolium-based ionic liquids. *Ind. Eng. Chem. Res.* **2013**, *52*, 18071−18075.
(24) Ji, Y. A.; Hou, Y. C.; Ren, S. H.; Yao, C. F.; Wu, W. Z. Highly efficient separation of phenolic compounds from oil mixtures by imidazolium-based dicationic ionic liquids via forming deep eutectic solvents. *Energy Fuels* **2017**, *31*, 10274−10282.
(25) Ji, Y. A.; Hou, Y. C.; Ren, S. H.; Yao, C. F.; Wu, W. Z. Highly efficient extraction of phenolic compounds from oil mixtures by trimethylamine-based dicationic ionic liquids via forming deep eutectic solvents. *Fuel Process. Technol.* **2018**, *171*, 183−191.
(26) Liu, Q.; Zhang, X. L.; Li, W. Separation of *m*-cresol from aromatic hydrocarbon and alkane using ionic liquids via hydrogen bond interaction. *Chin. J. Chem. Eng.* **2019**, *27*, 2675−2686.
(27) Xu, X.; Li, A.; Zhang, T.; Zhang, L. Z.; Xu, D. M.; Gao, J.; Wang, Y. L. Efficient extraction of phenol from low-temperature coal tar model oil via imidazolium-based ionic liquid and mechanism analysis. *J. Mol. Liq.* **2020**, *306*, 112911.
(28) Ranke, J.; Othman, A.; Fan, P.; Müller, A. Explaining ionic liquid water solubility in terms of cation and anion hydrophobicity. *Int. J. Mol. Sci.* **2009**, *10*, 1271−1289.
(29) Tian, G. C.; Feng, H. K.; Zhang, J. L. Study of effect of water on the physicochemical properties of 1-butyl-3-methylimidazolium chloride ionic liquids. *Adv. Mater. Res.* **2012**, *549*, 152−156.
(30) Ren, S. H.; Xiao, Y.; Wang, Y. M.; Kong, J.; Hou, Y. C.; Wu, W. Z. Effect of water on the separation of phenol from model oil with choline chloride via forming deep eutectic solvent. *Fuel Process. Technol.* **2015**, *137*, 104−108.
(31) Ji, Y. A.; Hou, Y. C.; Ren, S. H.; Yao, C. F.; Wu, W. Z. Tetraethylammonium amino acid ionic liquids and CO_2 for separation of phenols from oil mixtures. *Energy Fuels* **2018**, *32*, 11046−11054.
(32) Wong, D. S. H.; Chen, J. P.; Chang, J. M.; Chou, C. H. Phase equilibria of water and ionic liquids [emim][PF_6] and [bmim][PF_6]. *Fluid Phase Equilib.* **2002**, *194*, 1089−1095.
(33) Zhou, T.; Chen, L.; Ye, Y. M.; Chen, L. F.; Qi, Z. W.; Freund, H.; Sundmacher, K. An overview of mutual solubility of ionic liquids and water predicted by COSMO-RS. *Ind. Eng. Chem. Res.* **2012**, *51*, 6256−6264.
(34) Yao, C. F.; Hou, Y. C.; Sun, Y.; Wu, W. Z.; Ren, S. H.; Liu, H. Extraction of aromatics from aliphatics using a hydrophobic dicationic ionic liquid adjusted with small-content water. *Sep. Purif. Technol.* **2020**, *236*, 116287.
(35) Yao, C. F.; Hou, Y. C.; Ren, S. H.; Wu, W. Z.; Zhang, K.; Ji, Y. A.; Liu, H. Efficient separation of phenol from model oils using environmentally benign quaternary ammonium-based zwitterions via forming deep eutectic solvents. *Chem. Eng. J.* **2017**, *326*, 620−626.
(36) Song, Z.; Yu, D.; Zeng, Q.; Zhang, J. J.; Cheng, H. Y.; Chen, L. F.; Qi, Z. W. Effect of water on extractive desulfurization of fuel oils using ionic liquids: A COSMO-RS and experimental study. *Chin. J. Chem. Eng.* **2017**, *25*, 159−165.
(37) Gao, S. R.; Chen, X. C.; Abro, R.; Abdeltawab, A. A.; Al-Deyab, S. S.; Yu, G. R. Desulfurization of fuel oil: Conductor-like screening model for real solvents study on capacity of ionic liquids for thiophene and dibenzothiophene. *Ind. Eng. Chem. Res.* **2015**, *24*, 9421−9430.
(38) Cheng, H. Y.; Liu, C. Y.; Zhang, J. J.; Chen, L. F.; Zhang, B. J.; Qi, Z. W. Screening deep eutectic solvents for extractive desulfurization of fuel based on COSMO-RS model. *Chem. Eng. Process.* **2018**, *125*, 246−252.
(39) Salleh, Z.; Wazeer, I.; Mulyono, S.; El-blidi, L.; Hashim, M. A.; Hadj-Kali, M. K. Efficient removal of benzene from cyclohexane-benzene mixtures using deep eutectic solvents − COSMO-RS screening and experimental validation. *J. Chem. Thermodyn.* **2017**, *104*, 33−44.
(40) Eckert, F.; Klamt, A. Fast solvent screening via quantum chemistry: COSMO-RS approach. *AIChE J.* **2002**, *48*, 369−385.
(41) Klamt, A.; Eckert, F.; Arlt, W. COSMO-RS: an alternative to simulation for calculating thermodynamic properties of liquid mixtures. *Annu. Rev. Chem. Biomol.* **2010**, *1*, 101−122.
(42) Zhou, T.; Qi, Z. W.; Sundmacher, K. Model-based method for the screening of solvents for chemical reactions. *Chem. Eng. Sci.* **2014**, *115*, 177−185.
(43) Song, Z.; Zeng, Q.; Zhang, J. W.; Cheng, H. Y.; Chen, L. F.; Qi, Z. W. Solubility of imidazolium-based ionic liquids in model fuel hydrocarbons: A COSMO-RS and experimental study. *J. Mol. Liq.* **2016**, *224*, 544−550.
(44) Cheng, H. Y.; Li, J. S.; Wang, J. W.; Chen, L. F.; Qi, Z. W. Enhanced vitamin E extraction selectivity from deodorizer distillate by a biphasic system: A COSMO-RS and experimental study. *ACS Sustainable Chem. Eng.* **2018**, *6*, 5547−5554.
(45) Bai, Y. G.; Yan, R. Y.; Huo, F.; Qian, J. G.; Zhang, X. P.; Zhang, S. J. Recovery of methacrylic acid from dilute aqueous solutions by ionic liquids though hydrogen bonding interaction. *Sep. Purif. Technol.* **2017**, *184*, 354−364.
(46) Quijada-Maldonado, E.; van der Boogaart, S.; Lijbers, J. H.; Meindersma, G. W.; de Haan, A. B. Experimental densities, dynamic viscosities and surface tensions of the ionic liquids series 1-ethyl-3-methylimidazolium acetate and dicyanamide and their binary and ternary mixtures with water and ethanol at T = (298.15 to 343.15 K). *J. Chem. Thermodyn.* **2012**, *51*, 51−58.
(47) de la Parra, C. J.; Zambrano, J. R.; Bermejo, M. D.; Martín, Á.; Segovia, J. J.; Cocero, M. J. Influence of water concentration in the viscosities and densities of cellulose dissolving ionic liquids. Correlation of viscosity data. *J. Chem. Thermodyn.* **2015**, *91*, 8−16.
(48) Yao, C. Q.; Zhao, Y. C.; Chen, G. W. Multiphase processes with ionic liquids in microreactors: hydrodynamics, mass transfer and applications. *Chem. Eng. Sci.* **2018**, *189*, 340−359.
(49) Yao, C. F.; Hou, Y. C.; Ren, S. H.; Wu, W. Z.; Liu, H. Selective extraction of aromatics from aliphatics using dicationic ionic liquid-solvent composite extractants. *J. Mol. Liq.* **2019**, *291*, 111267.
(50) Klamt, A.; Eckert, F. COSMO-RS: a novel and efficient method for the a priori prediction of thermophysical data of liquids. *Fluid Phase Equilibr.* **2000**, *172*, 43−72.
(51) Lyu, Z. X.; Zhou, T.; Chen, L. F.; Ye, Y. M.; Sundmacher, K.; Qi, Z. W. Simulation based ionic liquid screening for benzene-cyclohexane extractive separation. *Chem. Eng. Sci.* **2014**, *113*, 45−53.

https://doi.org/10.1021/acsomega.1c04247
ACS Omega 2021, 6, 27368−27378

(52) Song, Z.; Zhou, T.; Zhang, J. N.; Cheng, H. Y.; Chen, L. F.; Qi, Z. W. Screening of ionic liquids for solvent-sensitive extraction −with deep desulfurization as an example. *Chem. Eng. Sci.* **2015**, *129*, 69−77.
(53) Song, Z.; Zhou, T.; Qi, Z. W.; Sundmacher, K. Systematic method for screening ionic liquids as extraction solvents exemplified by an extractive desulfurization process. *ACS Sustainable Chem. Eng.* **2017**, *5*, 3382−3389.
(54) Song, Z.; Hu, X. T.; Zhou, Y. G.; Zhou, T.; Qi, Z. W.; Sundmacher, K. Rational design of double salt ionic liquids as extraction solvents: Separation of thiophene/n-octane as example. *AIChE J.* **2019**, *65*, No. e16625.
(55) Hizaddin, H. F.; Ramalingam, A.; Hashim, M. A.; Hadj-Kali, M. K. O. Evaluating the performance of deep eutectic solvents for use in extractive denitrification of liquid fuels by the conductor-like screening model for real solvents. *J. Chem. Eng. Data* **2014**, *59*, 3470−3487.
(56) Hizaddin, H. F.; Sarwono, M.; Hashim, M. A.; Alnashef, I. M.; Hadj-Kali, M. K. Coupling the capabilities of different complexing agents into deep eutectic solvents to enhance the separation of aromatics from aliphatics. *J. Chem. Thermodyn.* **2015**, *84*, 67−75.
(57) Song, Z.; Zhang, J. J.; Zeng, Q.; Cheng, H. Y.; Chen, L. F.; Qi, Z. W. Effect of cation alkyl chain length on liquid-liquid equilibria of {ionic liquids + thiophene + heptane}: COSMO-RS prediction and experimental verification. *Fluid Phase Equilib.* **2016**, *425*, 244−251.
(58) Gao, S. R.; Yu, G. R.; Abro, R.; Abdeltawab, A. A.; Al-Deyab, S. S.; Chen, X. C. Desulfurization of fuel oils: Mutual solubility of ionic liquids and fuel oil. *Fuel* **2016**, *173*, 164−171.
(59) Gao, S. R.; Chen, X. C.; Abro, R.; Su, Z.; Abdeltawab, A. A.; Al-Deyab, S. S.; Yu, G. R. Mutual solubility of acidic ionic liquid and model gasoline of *n*-octane + 1-octene + toluene. *J. Taiwan Inst. Chem. Eng.* **2016**, *69*, 78−84.

https://doi.org/10.1021/acsomega.1c04247
ACS Omega 2021, 6, 27368−27378